Kinetochore components are required for central spindle assembly.

Gilliane Maton, Frances Edwards, Benjamin Lacroix, Marine Stefanutti, Kimberley Laband, Tiffany Lieury, Taekyung Kim, Julien Espeut, Julie C Canman, Julien Dumont

HHS Public Access

Author manuscript

Nat Cell Biol. Author manuscript; available in PMC 2016 May 01.

Published in final edited form as:

Nat Cell Biol. 2015 May ; 17(5): 697–705. doi:10.1038/ncb3150.

Kinetochore components are required for central spindle assembly

Gilliane Maton[1,*], **Frances Edwards**[1,*], **Benjamin Lacroix**[1], **Marine Stefanutti**[1], **Kimberley Laband**[1], **Tiffany Lieury**[1], **Taekyung Kim**[2], **Julien Espeut**[3], **Julie C. Canman**[4], and **Julien Dumont**[1,@]

[1]Institut Jacques Monod, CNRS, UMR 7592, University Paris Diderot, Sorbonne Paris Cité F-75205 Paris, France

[2]Ludwig Institute for Cancer Research/Department of Cellular and Molecular Medicine, University of California, San Diego, La Jolla, CA 92093 USA

[3]Université Montpellier, CRBM, CNRS UMR 5237, 34293 Montpellier, France

[4]Columbia University; Department of Pathology and Cell Biology, New York, NY 10033 USA

Abstract

A critical structure poised to coordinate chromosome segregation with division plane specification is the central spindle that forms between separating chromosomes after anaphase onset[1, 2]. The central spindle acts as a signaling center that concentrates proteins essential for division plane specification and contractile ring constriction[3]. However, the molecular mechanisms that control the initial stages of central spindle assembly remain elusive. Using *Caenorhabditis elegans* zygotes, we found that the microtubule bundling protein SPD-1^{PRC1} and the motor ZEN-4^{MKLP-1} are required for proper central spindle structure during its elongation[4-9]. By contrast, we found that the kinetochore controls the initiation of central spindle assembly. Specifically, central spindle microtubule assembly is dependent upon kinetochore recruitment of the scaffold protein KNL-1, as well as downstream partners BUB-1, HCP-1/2^{CENP-F}, and CLS-2^{CLASP}; and is negatively regulated by kinetochore-associated protein phosphatase 1 (PP1) activity. This in turn promotes central spindle localization of CLS-2^{CLASP} and initial central spindle microtubule assembly through its microtubule polymerase activity. Together, our results reveal an unexpected role for a conserved kinetochore protein network in coupling two critical events of cell division: chromosome segregation and cytokinesis.

[@]Corresponding author: dumont@ijm.univ-paris-diderot.fr.
[*]Equal contribution

Author Contributions: All experiments were conceived by J.D. with input from G.M. and F.E. Experiments were primarily performed and analyzed by G.M. and F.E. Biochemistry experiments were performed by B.L. Most of the transgenic strains used here were constructed by M.S. and K.L. T.L. developed the automated central spindle tracking and quantification software. T.K. constructed and provided the OD971 strain. J.C.C. and J.E. constructed and shared several strains used here. G.M., F.E., J.C.C. and J.D. made the figures and wrote the manuscript.

Competing Financial Interests: The authors declare no competing financial interests.

Keywords

Cytoskeleton; Kinetochore; Cell Division; Chromosome Segregation

The central spindle coordinates accurate chromosome segregation with division plane specification during cytokinesis, by acting as a hub for the localization of key regulators of these processes. Little is known about the initial stages of central spindle assembly and in particular how *de novo* central spindle microtubules assemble. In HeLa cells, *de novo* microtubule generation required for central spindle assembly is mediated in part by the Augmin complex, which promotes non-centrosomal microtubule nucleation during anaphase [2]. Importantly, this protein complex is not present in every species and no ortholog of any subunit has been identified in *C. elegans*. While the conserved microtubule bundling protein SPD-1^{PRC1} and the kinesin-6 motor ZEN-4^{MKLP1} are clearly required for proper central spindle structure, neither of these proteins appear to have microtubule nucleating or assembly promoting activity [10-12].

To study the initiation of central spindle assembly, we first developed an assay to quantify both central spindle microtubule density over time and overall central spindle mechanical integrity (see below) in the one-cell *C. elegans* embryo using both GFP-tagged TBB-2$^{\beta\text{-Tubulin}}$ and AIR-2^{AuroraB}, a component of the chromosomal passenger complex that strongly localizes to the central spindle in anaphase [13, 14]. We combined semi-automated GFP::TBB-2$^{\beta\text{-Tubulin}}$ and GFP::AIR-2^{AuroraB} intensity quantification over time with kymograph analysis of mCherry::HistoneH2B to track sister chromatid dynamics over time (Fig. 1a, b, c and Supplementary Fig. 1a, b).

Central spindle integrity has been attributed to the conserved microtubule bundling protein SPD-1^{PRC1} and the kinesin-6 motor ZEN-4^{MKLP1} (Fig. 1d). To determine if these proteins also play a role in the initiation of central spindle assembly, we monitored the assembly kinetics and mechanical integrity of the central spindle following RNAi mediated depletion. As expected, SPD-1^{PRC1} or ZEN-4^{MKLP1} depletion led to central spindle disruption and faster sister chromatid separation (Fig. 1e-i and Supplementary Video 1). Yet, in both SPD-1^{PRC1} and ZEN-4^{MKLP1} depleted embryos, a central spindle initially assembled but subsequently broke down into two half- or hemi-spindles connected to each set of rapidly separating chromatids (Fig. 1e, h). This rapid sister chromatid separation represents active cortical pulling forces acting on astral microtubules; forces that are normally counteracted by the central spindle, which slows down sister chromatid separation and limits the extent of segregation [15]. Thus faster sister chromatid separation reveals reduced central spindle mechanical integrity. To further demonstrate this, we repeated these experiments in the presence of reduced cortical pulling forces upon GPR-1 and -2 depletion. GPR-1/2 are required for cortically anchoring the minus end-directed motor Dynein, which in turn generates strong pulling forces on spindle poles. Strikingly, central spindle integrity was almost fully rescued in SPD-1^{PRC1} and ZEN-4^{MKLP1} depleted embryos when cortical pulling forces are reduced (Fig. 1j, k, Supplementary Fig. 1c and Video 2). These results suggest that SPD-1^{PRC1} and ZEN-4^{MKLP1} are not required for promoting initial central

spindle microtubule assembly but are essential for proper central spindle mechanical integrity during its elongation likely due to their role in microtubule crosslinking [1, 11, 12].

To identify components involved in initial anaphase central spindle assembly, we analyzed the potential contribution of the kinetochore, which participates in pre-anaphase spindle formation in most systems and has been associated with microtubule polymerizing activity [16]. To avoid the total failure of chromosome segregation that arises from full kinetochore inhibition following depletion of the core kinetochore scaffold protein KNL-1, we focused on the three sub-complexes/branches recruited downstream of KNL-1: RZZ/dynein (Rod, ZW10, Zwilch), Ndc80, and BUB-1 (Fig. 2a) [17]. To probe the roles of the RZZ/dynein and Ndc80 sub-complexes, the two main microtubule-binding entities at the kinetochore, we targeted ZWL-1^{ZWILCH} and NDC-80, respectively. To probe the role of the BUB-1 branch, which is involved in the spindle assembly checkpoint signaling and recruits microtubule associated proteins that control kinetochore microtubule dynamics (*e.g* CLS-2^{CLASP}), we targeted BUB-1 itself [18]. Inhibition of each sub-complex, through RNAi-mediated depletion of NDC-80, ZWL-1^{ZWILCH}, or BUB-1, led to chromosome mis-segregation events with frequent lagging chromosomes and anaphase chromatin bridges, as previously described (Supplementary Table 1) [19-21]. Interestingly, central spindle assembly was also dysregulated in all three RNAi conditions, demonstrating a post-anaphase role for kinetochores in central spindle formation and organization (Fig. 2b, c and Supplementary Video 3). ZWL-1^{ZWILCH}-depleted embryos had reduced GFP: :TBB-2$^{\beta\text{-Tubulin}}$ and GFP: :AIR-2^{AuroraB} in the central spindle region but showed normal sister chromatid separation kinetics, suggesting that central spindle mechanical integrity was not significantly affected (Fig. 2c-e). Zygotes treated with *ndc-80(RNAi)* exhibited elevated GFP: :AIR-2^{AuroraB} concentration on a smaller central spindle, likely due to reduced sister chromatid segregation caused by defective chromosome-microtubule end-on attachment (Fig. 2b, c) [22]. In contrast, the strongest phenotype was observed following BUB-1 depletion. First, *bub-1(RNAi)* zygotes had significantly faster and more extensive sister chromatid separation, suggesting that the mechanical integrity of the central spindle was highly impaired (Fig. 2d, e and Supplementary Table 1). Second, *bub-1(RNAi)* zygotes had lower levels of central spindle-associated GFP: :TBB-2$^{\beta\text{-Tubulin}}$ and GFP: :AIR-2^{AuroraB} combined with disorganized and disrupted central spindles (Fig. 2c, f and Supplementary Table 1). Thus *bub-1(RNAi)* zygotes displayed both of the defects expected from compromised central spindle assembly.

To further investigate the contribution of the BUB-1 branch to the initiation of central spindle assembly, we set out to determine whether proteins downstream of BUB-1 localize to the central spindle. During late prometaphase, BUB-1 kinase recruits two redundant CENP-F orthologs HCP-1 and -2 to the kinetochore, which in turn recruit the microtubule assembly regulator CLS-2^{CLASP} (Fig. 3a) [18, 23]. Interestingly, CLASP proteins have already been implicated in central spindle integrity in other systems [24, 25]. Immuno-localization of endogenous proteins and live imaging of GFP-tagged BUB-1, HCP-1$^{CENP\text{-}F}$ and CLS-2^{CLASP} revealed that all three components were transiently localized to the central spindle region shortly after anaphase onset (Fig. 3b, c). HCP-1$^{CENP\text{-}F}$ and CLS-2^{CLASP} were also detected in the spindle region throughout mitosis and CLS-2^{CLASP} concentrated at

spindle poles. We further found that the central spindle localization of CLS-2^{CLASP} during anaphase, but not its spindle pole targeting, was dependent on the presence of BUB-1 (Fig. 3c, Supplementary Fig. 2a). We next tested the functional significance of HCP-1/2^{CENP-F} and CLS-2^{CLASP} localization on the central spindle. Full depletion of HCP-1/2^{CENP-F} or CLS-2^{CLASP} led to a failure in chromosome biorientation coupled to premature spindle pole elongation and sister chromatid co-segregation to the same spindle pole (Fig. Supplementary Fig. 2b, c, Video 4 and Supplementary Table 1) [18]. In these embryos, a complete failure of central spindle assembly was observed (Supplementary Fig. 2c). Taken together, these results suggest that the BUB-1 kinetochore branch components relocalize to the central spindle during anaphase and are required for its initial assembly.

An alternative hypothesis is that failure of initial central spindle assembly could be due to the sister chromatid co-segregation to the same spindle pole observed in these embryos. Separation of sister chromatids to opposing spindle poles may be required for precise equatorial translocation of central spindle assembly factors between the chromosomes. To bypass any chromosome co-segregation defects, we performed a temporal dilution experiment by combining RNAi against HCP-1/2^{CENP-F} or CLS-2^{CLASP} with analysis of the first embryonic division after decreasing times following dsRNA injection. We identified a narrow temporal window during which sister chromatid alignment and co-segregation defects could be uncoupled from central spindle assembly in embryos with reduced levels of HCP-1/2^{CENP-F} or CLS-2^{CLASP} (Supplementary Fig. 2b, c and Video 4). Under these specific conditions, chromosomes aligned and segregated to opposite poles normally. However, the extent of sister chromatid and spindle pole segregation was still significantly greater than in control embryos, indicative of a loss of central spindle mechanical integrity (Fig. 3d-f, Supplementary Table 1 and Video 4 and 5). We also found microtubules and GFP: :AIR-2^{AuroraB} were absent from the central spindle region, indicative of a loss of central spindle assembly (Fig. 3g, h). These results not only demonstrated the crucial contribution of HCP-1/2^{CENP-F} and CLS-2^{CLASP} in central spindle microtubule assembly, they also highlight that this function requires higher protein levels than required for their role in chromosome alignment and separation to opposite spindle poles. Furthermore, in these embryos, and in contrast to SPD-1^{PRC1} or ZEN-4^{MKLP-1} depletion, the lack of a central spindle was evident immediately following anaphase onset and no hemi-spindle was visible (Fig. 1e, h vs 3d, g). Consistent with this, reducing cortical pulling forces by GPR-1/2 depletion in these embryos did not rescue central spindle assembly (Fig. 3i, j and Supplementary Video 2). Thus these results show that HCP-1/2^{CENP-F} and CLS-2^{CLASP} are essential for initiating central spindle microtubule assembly and suggests that their levels must be tightly controlled to avoid central spindle assembly defects.

We next tested if the initial metaphase kinetochore localization of these proteins is essential for the initiation of central spindle microtubule assembly during anaphase. Metaphase kinetochore targeting of BUB-1 requires the N-terminal half of KNL-1 via a series of eight phosphorylated MELT repeats [26-28]. Expression of an RNAi-resistant N-terminal truncation of KNL-1 (Δ85-505), that removes all eight MELTs, prevents kinetochore localization of BUB-1 when endogenous KNL-1 is absent (Fig. 4a) [29]. This truncation specifically disrupted the BUB-1 branch and did not lead to a complete disruption of the kinetochore, as GFP-tagged MIS-12 (Mis12 complex), KBP-4^{Spc24} (Ndc80 complex) and CZW-1^{ZW10}

(RZZ complex) all localized to the kinetochores, while BUB-1, HCP-1^{CENP-F} and CLS-2^{CLASP} did not (Fig. 4b, c, Supplementary Fig. 3 and 4). This mutant thus uncouples the recruitment of the three major kinetochore sub-complexes/branches downstream of KNL-1. Mutant embryos expressing KNL-1 Δ85-505 exhibited the same central spindle assembly defects as seen following depletion of BUB-1: sister chromatid separation was faster than in controls, and GFP: :TBB-2$^{\beta\text{-Tubulin}}$ and GFP: :AIR-2^{AuroraB} intensities were significantly decreased in the central spindle region (Fig. 4d-h). Additionally, the central spindle was completely disorganized and even broke apart (Fig. 4f, Supplementary Table 1 and Video 6). These results demonstrate that proper assembly of the kinetochore via KNL-1-dependent recruitment of BUB-1, HCP-1/2^{CENP-F} and CLS-2^{CLASP} during metaphase is required for the initiation of central spindle assembly after anaphase onset.

As reducing the overall levels of HCP-1/2^{CENP-F} or CLS-2^{CLASP} or preventing their kinetochore targeting reduced central spindle microtubule assembly and organization, we set out to test if increasing the level of these proteins at the kinetochores would likewise increase central spindle robustness. To test this, we used a KNL-1 mutant expected to recruit excess BUB-1 to the kinetochores. At the very N-terminus of KNL-1, an RRVSF motif acts as a kinetochore-docking site for protein phosphatase 1 (PP1), which in turn dephosphorylates the eight MELT repeats required for BUB-1 kinetochore localization (Fig. 4a) [30, 31]. As expected, we found that expression of an RNAi-resistant KNL-1 RRASA that prevents PP1 docking following endogenous KNL-1 depletion resulted in a two-fold increase in the level of kinetochore BUB-1: :GFP compared to controls (Supplementary Fig. 4a-c). This increase in BUB-1 at the metaphase kinetochores led to persistent localization of GFP: :HCP-1^{CENP-F} and CLS-2^{CLASP}: :GFP on the central spindle compared to control embryos (Fig. 4b, c and Supplementary Fig. 4d-h). Correspondingly, the kinetics of sister chromatid separation were slower in embryos expressing the KNL-1 RRASA mutant and this correlated with a significant increase in GFP: :TBB-2$^{\beta\text{-Tubulin}}$ and GFP: :AIR-2^{AuroraB} intensities in the central spindle region (Fig. 4d-h, Supplementary Table 1 and Video 6). Thus increasing the levels of BUB-1 on the kinetochores early in mitosis leads to persistent HCP-1^{CENP-F} and CLS-2^{CLASP} in the central spindle region, which initiates the assembly of a more robust central spindle in anaphase.

To test if this increase in central spindle intensity translated into improved mechanical integrity, we challenged the central spindle by enhancing astral microtubule-mediated cortical pulling forces. To do this, we depleted the kinesin-13 microtubule depolymerase KLP-7^{MCAK}, which leads to a dramatic increase in astral microtubule numbers and a corresponding increase in astral microtubule pulling forces [15, 32]. As expected, half of the central spindles that assembled in absence of KLP-7^{MCAK} broke apart and sister chromatids separated at a faster rate (Fig. 4f, i, j and Supplementary Video 7). Strikingly, both phenotypes were rescued in the KNL-1 RRASA mutant, consistent with these embryos having more robust central spindle assembly able to withstand abnormally elevated cortical pulling forces (Fig. 4i, j and Supplementary Video 7).

We next set out to determine how the kinetochore-dependent pathway promotes central spindle microtubule assembly. Secondary structure analysis of CLS-2^{CLASP} revealed three TOGL (Tumor Over-expressed Gene Like) domains characteristic of proteins with

microtubule assembly-promoting activity and involved in microtubule or tubulin heterodimer binding (Fig. 5a) [33]. To test if CLS-2^{CLASP} TOGL domains are functional, we performed an *in vitro* microtubule assembly assay in the presence of increasing concentration of recombinant CLS-2^{CLASP} purified from insect cells (Supplementary Fig. 5a). Increasing the concentration of recombinant CLS-2^{CLASP} displayed all three characteristics expected for a protein with microtubule polymerase activity: 1) shortening of the initial microtubule nucleation lag phase, 2) acceleration of microtubule assembly and 3) an increase of the steady-state plateau (Fig. 5b). To test if CLS-2^{CLASP} activity is required for central spindle assembly, we generated an RNAi-resistant CLS-2^{CLASP} mutant (CLS-2^{CLASP} W57A-K177A-R224A named hereafter CLS-2^{CLASP} 3A) impaired in TOGL1 tubulin heterodimer binding (Fig. 5a). Mutating these three residues is sufficient to dramatically reduce microtubule polymerase activity of TOGL domain-containing proteins without disrupting overall protein folding [34]. Strikingly, expression of the CLS-2^{CLASP} 3A mutant following endogenous CLS-2^{CLASP} partial depletion severely disrupted central spindle assembly and mechanical integrity (Fig. 5c-f, Supplementary Fig. 2d and Video 8). Altogether, these results demonstrate that kinetochores play an active role in promoting the initial assembly of a normal central spindle via PP1-modulated KNL-1-dependent recruitment of BUB-1, HCP-1/2^{CENP-F} and CLS-2^{CLASP} in metaphase. This early phase is required for their subsequent translocation in the central spindle region at anaphase onset, which in turn promotes initial central spindle microtubule assembly through CLS-2^{CLASP} activity.

Here we have identified a new unexpected role for the kinetochore in driving central spindle assembly. We propose a model in which the central spindle is formed by a two-stage process (Fig. 5j). In the first stage, the newly identified kinetochore pathway promotes the initiation of *de novo* microtubule assembly between the segregating sister chromatids via CLS-2^{CLASP} activity. In the second stage, the microtubule bundling proteins SPD-1^{PRC1} and ZEN-4^{MKLP1} promote central spindle elongation and proper microtubule organization. In support of this model, GFP: :EBP-1^{EB1} imaging revealed an initial burst of microtubule assembly in the central spindle region within seconds after anaphase onset, which was associated with peak levels of CLS-2^{CLASP} in the region (Fig. 5g-I, Supplementary Fig. 5b and Video 9 and 10). Accordingly, the GFP: :EBP-1^{EB1} burst was abrogated by CLS-2^{CLASP} depletion or expression of KNL-1(Δ85-505), and increased following KNL-1 RRASA expression (Fig. 5g, h). We also found SPD-1^{PRC1} was recruited to the central spindle later, after the initial structure was formed, consistent with a role in the second stage and not the first stage of central spindle assembly (Fig. 5i and Supplementary Fig. 5b). Moreover, we found that in *C. elegans* zygotes, CLS-2^{CLASP} recruitment to the central spindle was independent of SPD-1^{PRC1} (Fig. 5c, d) [25]. Finally, we observed hemi-spindles connected to the segregating chromatids following SPD-1^{PRC1} or ZEN-4^{MKLP1} RNAi but not in BUB-1, HCP-1/2^{CENP-F}, or CLS-2^{CLASP} depleted embryos (Fig. 1e, h and 3d, g). Thus we have uncovered a novel role for a subset of kinetochore proteins in promoting and regulating the initiation of central spindle assembly, and potentially coupling the two most critical events of cell division: chromosome segregation and cytokinesis (Fig. 5j). Because kinetochore components and the central spindle are highly conserved throughout metazoans, the mechanisms elucidated here are likely to be conserved in vertebrates.

Supplementary Material

Refer to Web version on PubMed Central for supplementary material.

Acknowledgments

We thank all members of the Tran/Paoletti, Pintard, Doye and Dumont labs for support and advice. We are grateful to Patricia Moussounda and Patricia Feynerol for providing technical support. We thank Carsten Janke and Nicolas Tavernier for their help with protein purification. We thank Arshad Desai and the CGC for worm strains. We thank Yuji Kohara for the zen-4^{MKLP1} cDNA (yk35d10). We are grateful to Mimi Shirasu-Hiza for critical reading of the manuscript. T.K. is supported by R01-GM074215 (awarded to A. Desai). This work was supported by grants from the ANR (ANR-09-RPDOC-005-01), the FRM (AJE201112) and the Mairie de Paris (Emergence) to J.D., and NIH DP2 OD008773 to J.C.C.

References

1. Lee KY, Davies T, Mishima M. Cytokinesis microtubule organisers at a glance. Journal of Cell Science. 2012; 125:3495–3500. [PubMed: 22991411]
2. Uehara R, Goshima G. Functional central spindle assembly requires de novo microtubule generation in the interchromosomal region during anaphase. The Journal of Cell Biology. 2010
3. Glotzer M. The molecular requirements for cytokinesis. Science. 2005; 307:1735–1739. [PubMed: 15774750]
4. Raich WB, Moran AN, Rothman JH, Hardin J. Cytokinesis and midzone microtubule organization in Caenorhabditis elegans require the kinesin-like protein ZEN-4. Mol Biol Cell. 1998; 9:2037–2049. [PubMed: 9693365]
5. Verbrugghe KJ, White JG. SPD-1 is required for the formation of the spindle midzone but is not essential for the completion of cytokinesis in C. elegans embryos. Current biology : CB. 2004; 14:1755–1760. [PubMed: 15458647]
6. Schuyler SC, Liu JY, Pellman D. The molecular function of Ase1p: evidence for a MAP-dependent midzone-specific spindle matrix. Microtubule-associated proteins. J Cell Biol. 2003; 160:517–528. [PubMed: 12591913]
7. Jiang W, et al. PRC1: a human mitotic spindle-associated CDK substrate protein required for cytokinesis. Mol Cell. 1998; 2:877–885. [PubMed: 9885575]
8. Mollinari C, et al. PRC1 is a microtubule binding and bundling protein essential to maintain the mitotic spindle midzone. J Cell Biol. 2002; 157:1175–1186. [PubMed: 12082078]
9. Powers J, Bossinger O, Rose D, Strome S, Saxton W. A nematode kinesin required for cleavage furrow advancement. Curr Biol. 1998; 8:1133–1136. [PubMed: 9778533]
10. Hu CK, Ozlu N, Coughlin M, Steen JJ, Mitchison TJ. Plk1 negatively regulates PRC1 to prevent premature midzone formation before cytokinesis. Mol Biol Cell. 2012; 23:2702–2711. [PubMed: 22621898]
11. Subramanian R, et al. Insights into Antiparallel Microtubule Crosslinking by PRC1, a Conserved Nonmotor Microtubule Binding Protein. Cell. 2010; 142:433–443. [PubMed: 20691902]
12. Bieling P, Telley IA, Surrey T. A Minimal Midzone Protein Module Controls Formation and Length of Antiparallel Microtubule Overlaps. Cell. 2010; 142:420–432. [PubMed: 20691901]
13. Carmena M, Wheelock M, Funabiki H, Earnshaw WC. The chromosomal passenger complex (CPC): from easy rider to the godfather of mitosis. Nature reviews Molecular cell biology. 2012; 13:789–803. [PubMed: 23175282]
14. van der Horst A, Lens SM. Cell division: control of the chromosomal passenger complex in time and space. Chromosoma. 2014; 123:25–42. [PubMed: 24091645]
15. Grill SW, Gönczy P, Stelzer EH, Hyman AA. Polarity controls forces governing asymmetric spindle positioning in the Caenorhabditis elegans embryo. Nature. 2001; 409:630–633. [PubMed: 11214323]
16. Cheeseman IM. The Kinetochore. Cold Spring Harbor perspectives in biology. 2014; 6

17. Desai A, et al. KNL-1 directs assembly of the microtubule-binding interface of the kinetochore in C. elegans. Genes & development. 2003; 17:2421–2435. [PubMed: 14522947]
18. Cheeseman IM, MacLeod I, Yates JR 3rd, Oegema K, Desai A. The CENP-F-like proteins HCP-1 and HCP-2 target CLASP to kinetochores to mediate chromosome segregation. Curr Biol. 2005; 15:771–777. [PubMed: 15854912]
19. Oegema K, Desai A, Rybina S, Kirkham M, Hyman AA. Functional analysis of kinetochore assembly in Caenorhabditis elegans. J Cell Biol. 2001; 153:1209–1226. [PubMed: 11402065]
20. Cheeseman IM, et al. A conserved protein network controls assembly of the outer kinetochore and its ability to sustain tension. Genes Dev. 2004; 18:2255–2268. [PubMed: 15371340]
21. Gassmann R, et al. A new mechanism controlling kinetochore-microtubule interactions revealed by comparison of two dynein-targeting components: SPDL-1 and the Rod/Zwilch/Zw10 complex. Genes & Development. 2008; 22:2385–2399. [PubMed: 18765790]
22. Cheeseman IM, Chappie JS, Wilson-Kubalek EM, Desai A. The conserved KMN network constitutes the core microtubule-binding site of the kinetochore. Cell. 2006; 127:983–997. [PubMed: 17129783]
23. Essex A, Dammermann A, Lewellyn L, Oegema K, Desai A. Systematic analysis in Caenorhabditis elegans reveals that the spindle checkpoint is composed of two largely independent branches. Molecular biology of the cell. 2009; 20:1252–1267. [PubMed: 19109417]
24. Inoue YH, et al. Mutations in orbit/mast reveal that the central spindle is comprised of two microtubule populations, those that initiate cleavage and those that propagate furrow ingression. The Journal of Cell Biology. 2004; 166:49–60. [PubMed: 15240569]
25. Liu J, et al. PRC1 cooperates with CLASP1 to organize central spindle plasticity in mitosis. The Journal of biological chemistry. 2009; 284:23059–23071. [PubMed: 19561070]
26. Krenn V, Overlack K, Primorac I, Van Gerwen S, Musacchio A. KI Motifs of Human Knl1 Enhance Assembly of Comprehensive Spindle Checkpoint Complexes around MELT Repeats. Current Biology. 2014; 24:29–39. [PubMed: 24361068]
27. Vleugel M, et al. Arrayed BUB recruitment modules in the kinetochore scaffold KNL1 promote accurate chromosome segregation. J Cell Biol. 2013; 203:943–955. [PubMed: 24344183]
28. Zhang G, Lischetti T, Nilsson J. A minimal number of MELT repeats supports all the functions of KNL1 in chromosome segregation. J Cell Sci. 2014; 127:871–884. [PubMed: 24363448]
29. Moyle MW, et al. A Bub1-Mad1 interaction targets the Mad1-Mad2 complex to unattached kinetochores to initiate the spindle checkpoint. J Cell Biol. 2014; 204:647–657. [PubMed: 24567362]
30. Espeut J, Cheerambathur DK, Krenning L, Oegema K, Desai A. Microtubule binding by KNL-1 contributes to spindle checkpoint silencing at the kinetochore. The Journal of cell biology. 2012; 196:469–482. [PubMed: 22331849]
31. London N, Biggins S. Mad1 kinetochore recruitment by Mps1-mediated phosphorylation of Bub1 signals the spindle checkpoint. Genes & Development. 2014; 28:140–152. [PubMed: 24402315]
32. Srayko M, Kaya A, Stamford J, Hyman AA. Identification and characterization of factors required for microtubule growth and nucleation in the early C. elegans embryo. Developmental cell. 2005; 9:223–236. [PubMed: 16054029]
33. Al-Bassam J, Chang F. Regulation of microtubule dynamics by TOG-domain proteins XMAP215/Dis1 and CLASP. Trends in cell biology. 2011; 21:604–614. [PubMed: 21782439]
34. Funk C, Schmeiser V, Ortiz J, Lechner J. A TOGL domain specifically targets yeast CLASP to kinetochores to stabilize kinetochore microtubules. J Cell Biol. 2014; 205:555–571. [PubMed: 24862575]

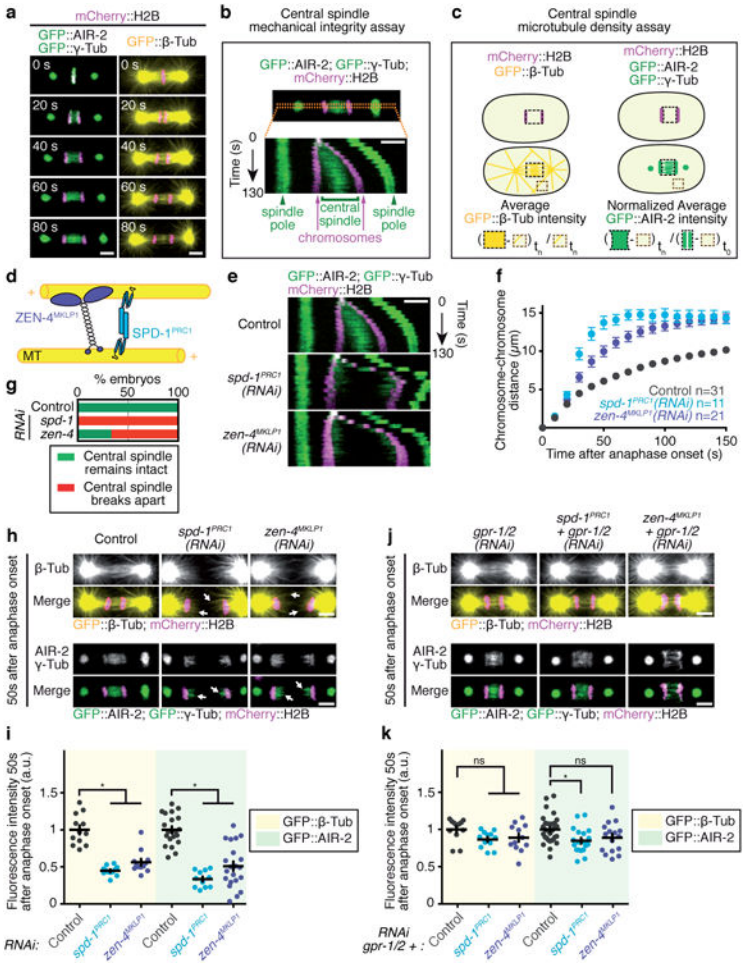

Figure 1. SPD-1^{PRC1} and ZEN-4^{MKLP1} are required for central spindle stabilization and bundling

(a) Central spindle assembly in the indicated strains. Timings are relative to anaphase onset. **(b)** Kymographic assay for central spindle mechanical integrity analysis. **(c)** Functional assay for central spindle density analysis. **(d)** Schematics of SPD-1^{PRC1} and ZEN-4^{MKLP1} binding to overlapping microtubule plus-ends. **(e)** Kymographs for the indicated conditions. **(f)** Chromosome to chromosome distance after anaphase onset for the indicated conditions. The sample size (number of embryos analyzed) is provided in the figure and was generated by aggregation over 3 independent experiments. Error bars represent the SEM. **(g)** Percentage of one-cell embryos that displayed a breaking apart central spindle in the indicated conditions. **(h)** Central spindle assembly and phenotypes for the indicated conditions. The white arrows indicate the presence of remaining microtubules connected to each set of separating sister chromatids and that initially formed at the central spindle before it broke apart. **(i)** Quantification of central spindle intensity after *spd-1^{PRC1}(RNAi)* (GFP: :β-Tub, p<0.0001; GFP: :AIR-2, p<0.0001) and *zen-4^{MKLP1}(RNAi)* (GFP: :β-Tub, p<0.0001; GFP: :AIR-2, p<0.0001). The mean is shown for n=31, 11 and 21 embryos for control, *spd-1(RNAi)* and *zen-4(RNAi)*, respectively. Data was aggregated over 3 independent experiments. One-way ANOVA was used to determine significance. **(j)** Central spindle assembly and phenotypes for the indicated conditions. **(k)** Quantification of central spindle

intensity after *gpr-1/2+spd-1*^{PRC1}*(RNAi)* (GFP: :β-Tub, p=0.0750; GFP: :AIR-2, p=0.0103) and *gpr-1/2+zen-4*^{MKLP1}*(RNAi)* (GFP: :β-Tub, p=0.1578; GFP: :AIR-2, p=0.1047). The mean is shown for n=31, 20 and 16 embryos for *gpr-1/2(RNAi)*, *gpr-1/2+spd-1(RNAi)* and *gpr-1/2+zen-4(RNAi)*, respectively. Data was aggregated over 3 independent experiments. One-way ANOVA was used to determine significance. Error bars

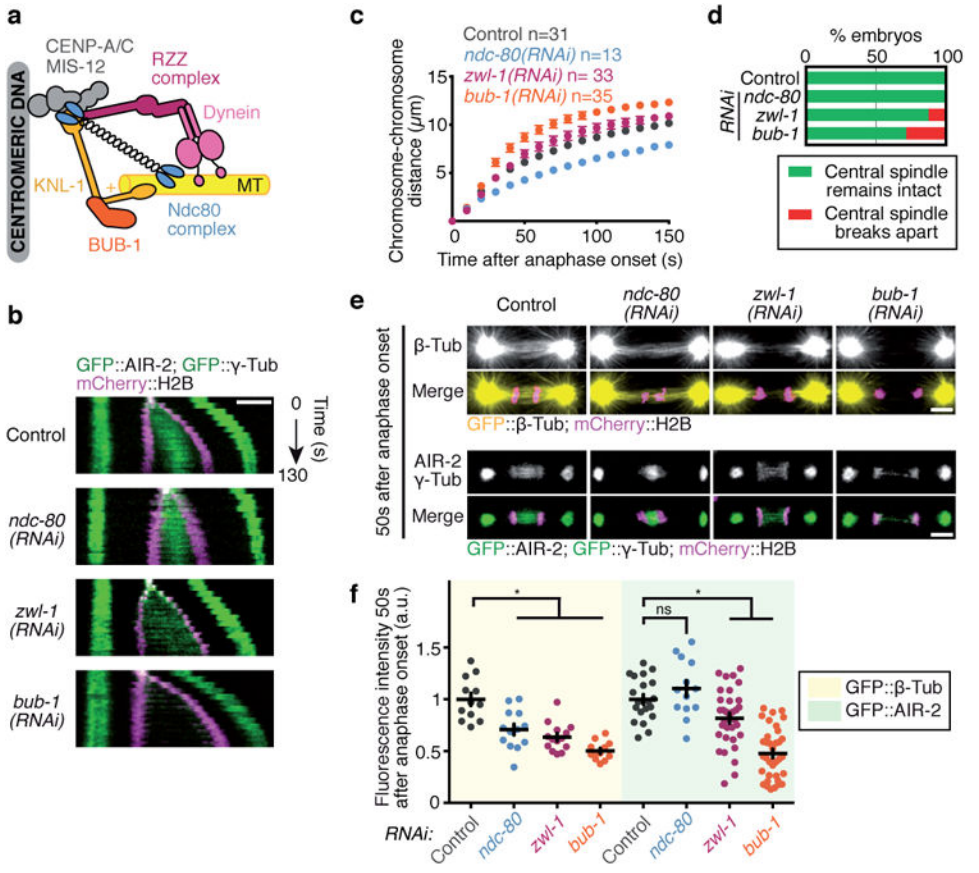

Figure 2. A subset of kinetochore proteins are involved in central spindle assembly

(a) Schematics of kinetochore sub-complexes analyzed. **(b)** Kymographs for the indicated conditions. **(c)** Chromosome to chromosome distance after anaphase onset for the indicated conditions. The sample size (number of embryos analyzed) is provided in the figure and was generated by aggregation over 3 independent experiments. Error bars represent the SEM. **(d)** Percentage of one-cell embryos that displayed a breaking apart central spindle in the indicated conditions. **(e)** Central spindle assembly and phenotypes for the indicated conditions. **(f)** Quantification of central spindle intensity after *ndc-80(RNAi)* (GFP: :β-Tub, p<0.0001; GFP: :AIR-2, p=0,7065), *zwl-1* ^{ZWILCH}*(RNAi)* (GFP: :β-Tub, p<0.0001; GFP: :AIR-2, p=0.0417) and *bub-1(RNAi)* (GFP: :β-Tub, p<0.0001; GFP: :AIR-2, p<0.0001). The mean is shown for n=31, 13, 33 and 35 embryos for control, *ndc-80(RNAi)*, *zwl-1(RNAi)* and *bub-1(RNAi)*, respectively. Data was aggregated over 3 independent experiments. One-way ANOVA was used to determine significance. Error bars represent the SEM. Scale bars, 5 μm.

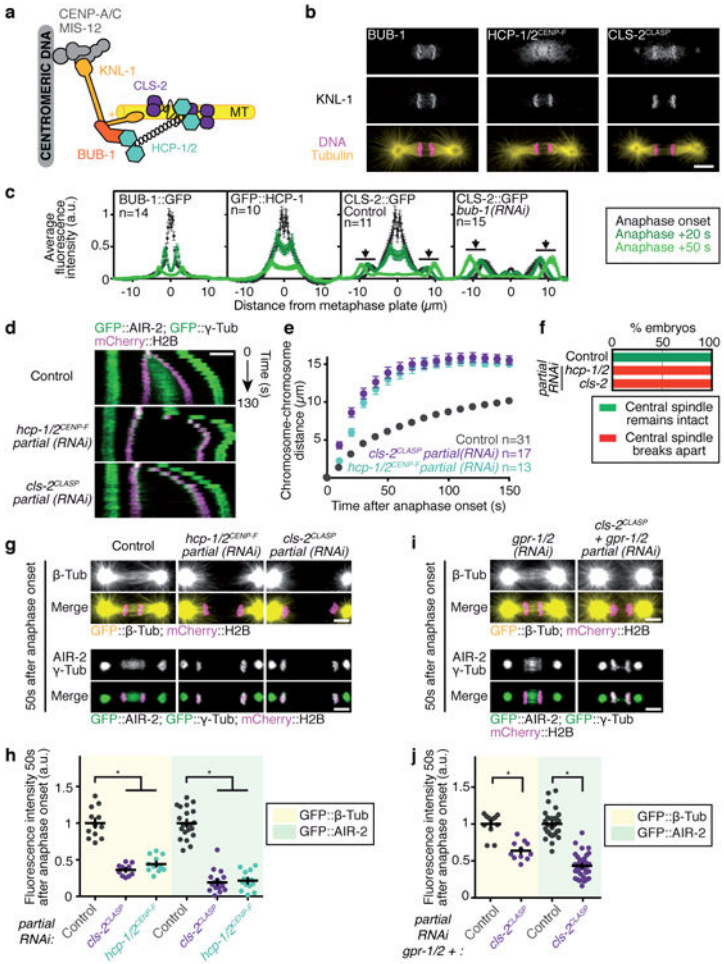

Figure 3. The BUB-1/HCP-1/2^{CENPF}/CLS-2^{CLASP} pathway is essential for initiating central spindle formation

(a) Schematics of components of the BUB-1 kinetochore branch. **(b)** Fixed control embryos were stained to visualize DNA, α-Tubulin, BUB-1, HCP-1/2^{CENP-F}, CLS-2^{CLASP} and KNL-1 in anaphase. **(c)** Fluorescence intensity for indicated GFP-tagged proteins along the central spindle at anaphase onset (black dots), and 20 or 50 seconds after anaphase onset (respectively dark and light green dots). 0 μm corresponds to the position of chromosomes at anaphase onset. Black arrows indicate the spindle pole localization of CLS-2^{CLASP}. The sample size (number of embryos analyzed) is provided in the figure and was generated by aggregation over 2 independent experiments. Error bars represent the SEM. **(d)** Kymographs for the indicated conditions. **(e)** Chromosome to chromosome distance after anaphase onset for the indicated conditions. Chromosome to chromosome distance after anaphase onset for the indicated conditions. The sample size (number of embryos analyzed) is provided in the figure and was generated by aggregation over 3 independent experiments. Error bars represent the SEM. **(f)** Percentage of one-cell embryos that displayed a breaking apart central spindle in the indicated conditions. **(g)** Central spindle assembly and phenotypes for the indicated conditions. **(h)** Quantification of central spindle intensity after *cls-2^{CLASP}(RNAi)* (GFP: :β-Tub, p=<0.0001; GFP: :AIR-2, p<0.0001) and *hcp-1/2^{CENP-F}(RNAi)* (GFP: :β-Tub, p=<0.0001; GFP: :AIR-2, p<0.0001). The mean is

shown for n=31, 17 and 13 embryos for control, *cls-2(RNAi)* and *hcp-1/2 (RNAi)*, respectively. Data was aggregated over 3 independent experiments. One-way ANOVA was used to determine significance. Error bars represent the SEM. **(i)** Central spindle assembly and phenotypes for the indicated conditions. **(j)** Quantification of central spindle intensity after *gpr-1/2+cls-2*^{CLASP}*(RNAi)* (GFP: β-Tub, p<0.0001; GFP: AIR-2, p<0.0001). The mean is shown for n=31 and 17 embryos for *gpr-1/2(RNAi)* and *gpr-1/2+cls-2(RNAi)* respectively. Data was aggregated over 3 independent experiments. One-way ANOVA was used to determine significance. Error bars represent the SEM. Scale bars, 5 μm.

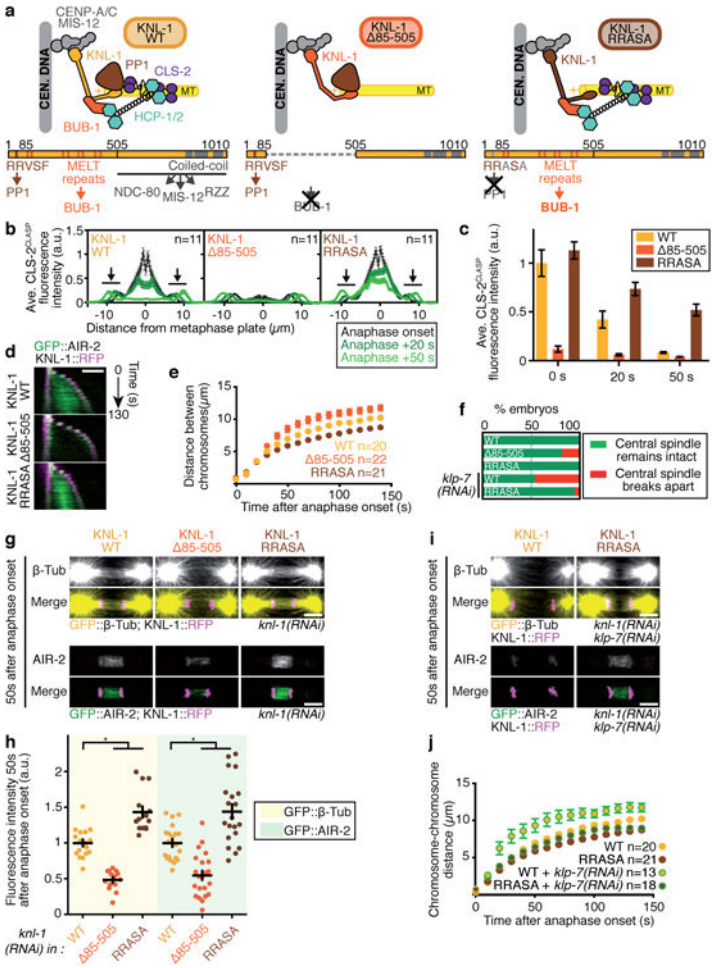

Figure 4. PP1-modulated KNL-1-dependent recruitment of BUB-1/HCP-1/2^{CENP-F}/CLS-2^{CLASP} controls central spindle assembly

(a) Schematics of mutations engineered in KNL-1. **(b)** Fluorescence intensity of GFP-tagged CLS-2 along the central spindle at anaphase onset (black dots), and 20 or 50 seconds after anaphase onset (respectively dark and light green dots) in indicated KNL-1 mutants. All experiments were performed in absence of endogenous KNL-1. 0 μm corresponds to the position of chromosomes at anaphase onset. Black arrows indicate the spindle pole localization of CLS-2^{CLASP}. The sample size (number of embryos analyzed) is provided in the figure and was generated by aggregation over 2 independent experiments. Error bars represent the SEM. **(c)** Quantification of average CLS-2^{CLASP} fluorescence intensity centred on chromosome position at anaphase onset. Each value is normalized against the WT average intensity at 0 s. Error bars represent the SEM. **(d)** Kymographs for the indicated conditions. **(e)** Chromosome to chromosome distance after anaphase onset for the indicated conditions. The sample size (number of embryos analyzed) is provided in the figure and was generated by aggregation over 3 independent experiments. Error bars represent the SEM. **(f)** Percentage of one-cell embryos that displayed a breaking apart central spindle in the indicated conditions. **(g)** Central spindle assembly and phenotypes for the indicated conditions. **(h)** Quantification of central spindle intensity in KNL-1 A85-505 (GFP: :β-Tub, $p<0.0001$; GFP: :AIR-2, $p=0.0002$) and KNL-1 RRASA (GFP: :β-Tub, $p<0.0001$;

GFP: :AIR-2, p=0.0003). The mean is shown for n=20, 22 and 21 embryos for KNL-1 WT, KNL-1 Δ85-505 and KNL-1 RRASA respectively. Data was aggregated over 3 independent experiments. One-way ANOVA was used to determine significance. **(i)** Central spindle assembly and phenotypes for the indicated conditions. **(j)** Chromosome to chromosome distance after anaphase onset for the indicated conditions. The sample size (number of embryos analyzed) is provided in the figure and was generated by aggregation over 3 independent experiments. Error bars represent the SEM. Scale bars, 5 μm.

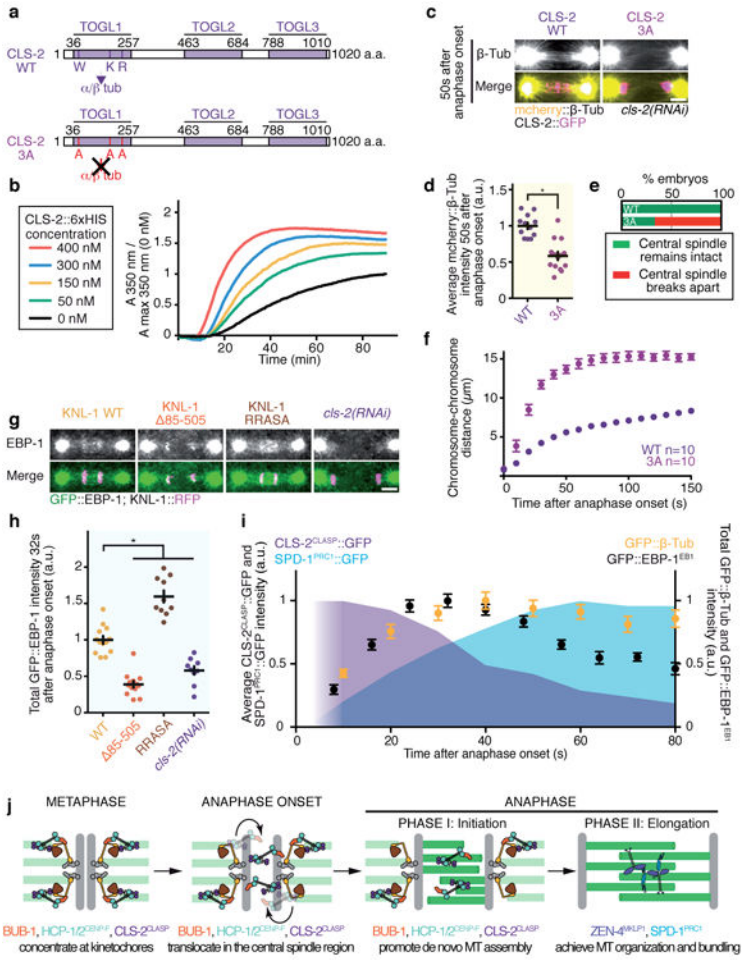

Figure 5. CLS-2^{CLASP} activity is required for central spindle assembly and a two-stage model of central spindle organization

(a) Schematics of CLS-2^{CLASP} domain organization and engineered mutations. **(b)** Microtubule polymerization timecourses with indicated concentrations of CLS-2^{CLASP}: :6xHIS. Data shown represent one out of 3 independent experiments. **(c)** Central spindle assembly and phenotypes for the indicated conditions. **(d)** Quantification of central spindle intensity in CLS-2^{CLASP} WT and CLS-2^{CLASP} 3A ($p<0.0001$). The mean is shown for n=10 embryos in each condition. Data was aggregated over 3 independent experiments. A Student t-test was used to determine significance. **(e)** Percentage of one-cell embryos that displayed a breaking apart central spindle in the indicated conditions. **(f)** Chromosome to chromosome distance after anaphase onset for the indicated conditions. The sample size (number of embryos analyzed) is provided in the figure and was generated by aggregation over 3 independent experiments. Error bars represent the SEM. **(g)** GFP-tagged EBP-1^{EB1} localization at the central spindle in the indicated conditions. **(h)** Quantification of EBP-1^{EB1} intensity at the central spindle intensity in KNL-1 WT, KNL-1 Δ85-505 ($p<0.0001$), KNL-1 RRASA ($p<0.0001$) and *cls-2^{CLASP}(RNAi)* ($p<0.0001$). The mean is shown for n=13, 13, 10 and 10 embryos for KNL-1 WT, KNL-1 Δ85-505, KNL-1 RRASA and *cls-2(RNAi)* respectively. Data was aggregated over 3 independent experiments. One-way ANOVA was used to determine significance. **(i)** Quantification of average

(CLS-2^{CLASP} and SPD-1^{PRC1}, between 10 and 80 sec after anaphase onset) or total (β-tubulin and EBP-1^{EB1}, between 8 and 80 sec after anaphase onset) fluorescence intensity at the central spindle over time. The mean is shown for n=13, 12, 13 and 11 embryos for GFP: :β-Tub, CLS-2: :GFP, SPD-1: :GFP and EBP-1: :GFP respectively. Data was aggregated over 2 independent experiments. Error bars represent the SEM. **(j)** A two-stage model of central spindle organization. BUB-1, HCP-1/2^{CENP-F} and CLS-2^{CLASP} are concentrated at the kinetochore during metaphase in a KNL-1-dependent manner opposed by PP1 activity. This concentration allows their timely translocation in the central spindle region at anaphase onset. Central spindle localized CLS-2^{CLASP} promotes microtubule formation via its microtubule assembly promoting activity. As CLS-2^{CLASP} leaves the central spindle region, SPD-1^{PRC1} and ZEN-4^{MKLP1} accumulate and, through their microtubule cross-linking activity, stabilize the central spindle during its elongation. Scale bars, 5 μm.